

Paper:

# Rate and Temperature Dependent Hysteresis Online Identification for Magnetostrictive Actuator

Sicheng Yi<sup>1,2</sup>, Yuchao Yan<sup>1</sup>, Huijun Fan<sup>3</sup>, Quan Zhang<sup>2</sup>

1 Shanghai Aerospace Control Technology Institute, 2 Shanghai University, 3 Baoding Cigarette Factory

E-mail: lincolnquan@shu.edu.cn

[Received 00/00/00; accepted 00/00/00]

**An online model identification approach is proposed to describe the rate/temperature hysteresees for magnetostrictive actuator in this article. Magnetostrictive hysteresis loops show asymmetric, rate-dependent phenomena under different input currents and experimental temperatures. It is difficult to apply a comprehensive model to accurately capture such hysteresis variation. The hysteresis offline identification study is conducted. However, the rate/temperature-dependent hysteresis cannot be described well via the offline method, due to the unmodeled dynamics and external disturbances. To this end, the online infinite impulse response (OIIR) and fractional order polynomial modified Prandtl Ishlinskii (FPMPI) integrated model is utilized for the rate/temperature-dependent hysteresis identification. Comparison of the online and offline identification results shows that the hysteresis online identification results are typically better than the offline results, at the level of one order of magnitude.**

**Keywords:** Online identification, magnetostrictive, rate/temperature-dependent, hysteresis

## 1. Introduction

Magnetostrictive actuator is progressively being investigated for micropositioning and microvibration control applications where fast reaction, large powers density, high resolution are required. However, for the magnetostrictive actuator, the output vs. input loops exhibit complicated hysteresis phenomena, which tend to be asymmetric, saturate, and dynamic [1]. The profile of hysteresis loop is dependent on the amplitude/frequency/bias of the input signal and surrounding temperature, etc. To predict the response, it is essential to exactly formulate the hysteresis model.

As to the rate-independent hysteresis model, the physical and phenomenological [2] approaches have been extensively reported. The typical phenomenological modeling approaches include neural network (NN) [3], the Krasnosel'skii Pokrovskii (KP) [4], Preisach [5], and Prandtl Ishlinskii (PI) like [6] modeling approaches. PI-like model possesses a more simplified form compared

against the KP and Preisach models. In terms of those PI-like models, different Lipschitz continuous functions, e.g. integer order polynomial [7, 8], hyperbolic tangent [9], Sigmoid function [10], are applied to modify the conventional Play operator. The modified PI model can be used for asymmetric hysteresis modeling.

It is difficult to build the rate-dependent hysteresis model over a wide range of frequency. To the best of our knowledge, three kinds of approaches are proposed in the previous studies. (i) The conventional hysteresis operators are modified [11–13]. In most cases, the weight or threshold function is changed to be rate-dependent. However, the rate-dependent threshold function needs to hold the dilation condition. Moreover, the developed model is only effective when the input signal covers narrow frequency bandwidth. (ii) Some intelligent models based on fuzzy or machine learning theory are proposed to describe the rate-dependent hysteresis [14–16]. However, the complicated intelligent algorithms are required to realize rate-dependent hysteresis modeling. (iii) A few hysteresis models based on the Hammerstein principle are presented [17–19]. However, whether the rate-independent hysteresis or rate-dependent dynamics is identified offline. The system uncertainty not considered for the hysteresis offline modeling approach may result in unmodeled error.

The temperature also plays effect upon the hysteresis of the magnetostrictive and other smart material actuators. The hysteresis characterizations of the piezo-stack actuator for different temperatures are studied experimentally [20, 21]. It is concluded that the basic shape of the hysteresis loop is free from temperature, but the displacement and sensitivity (mean slope) of the hysteresis increase with the growing surrounding temperature. A few studies have been performed to model the temperature-dependent hysteresis. A temperature-dependent Prandtl Ishlinskii model (TD-PI) is proposed to account for the temperature effects on the hysteresis nonlinearity [20]. For the TD-PI model, a temperature-shape function is integrated into the traditional PI model. However, the determination of temperature-shape function is a difficult problem. A model, incorporating the thermal and piezoelectric sub-models, is presented [21]. However, the thermal sub-model is established by the FEM method, resulting in a lot of computation for model identification.

It motivates us to propose a proper hysteresis modeling

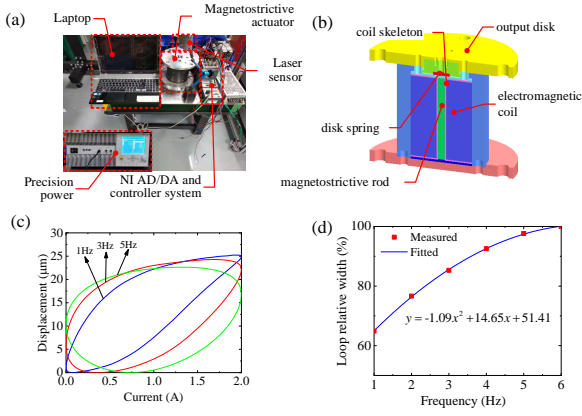


**Fig. 1.** Experimental characterization of the rate-dependent output vs. input loops for the magnetostrictive actuator: (a) experimental setup; (b) CAD model of the actuator cross-section; (c) measured rate-dependent hystereses; (d) loop relative width vs. input frequency.

approach to capture the rate and temperature effects of the hysteresis[22]. It is a big challenge to establish and identify a hysteresis model totally incorporating those factors. First, the dimensions of model parameters are large; secondly, it is complex to build large data sets for purpose of describing the evolving hysteresis offline. To address this issue, an online identification approach capable of tracking the actual rate/temperature-dependent hysteretic response is presented in this paper.

## 2. Rate/temperature-dependent hysteresis

The rate-dependent property of the magnetostrictive hysteresis is illustrated in Fig. 1. The experimental setup and cross-section of the CAD model are shown in Fig. 1(a) and Fig. 1(b) respectively. The output vs. input loops of the magnetostrictive actuator are shown in Fig. 1(c), when the 2 A currents of different frequencies are utilized to drive the magnetostrictive actuator. It is seen that as the input frequencies raise, the loop relative widths increase and the maximum displacements of the magnetostrictive actuator decrease. Fig. 1(d) shows the quantitative results of the loop relative widths from 1 Hz to 5 Hz. The definition of the loop relative width is the ratio of the loop maximum width to the maximum displacement. It is also found that the relationship of loop relative width vs. frequency can be well fitted by a monotonously increasing quadratic polynomial function.

Another custom-developed magnetostrictive micropositioner (see Fig. 2(a)) is utilized to examine the temperature-dependent characteristics of the output vs. input loops. The stroke of the magnetostrictive actuator is magnified by an amplified structure which is essentially a lever arm. The reason we use this magnetostrictive micropositioner is that its diameter is smaller than the one in Fig. 2(a), making it easier to measure the temperature of

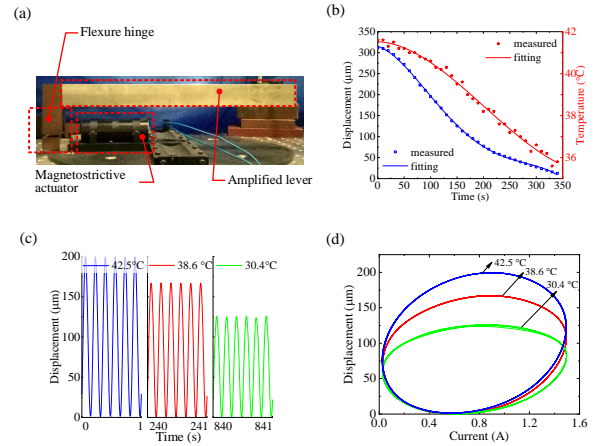


**Fig. 2.** Experimental characterization of the temperature-dependent output vs. input loops for the magnetostrictive micropositioner: (a) experimental setup; (b) measured and fitting displacement vs. time, and temperature vs. time respectively; (c) output displacements with 6 Hz input current under different surrounding temperatures; (d) temperature-dependent hysteresis loops.

the actuator housing and thus evaluate heat changes inside the actuator.

When the surrounding temperature of the magnetostrictive material rises, the additional thermal-induced strain is produced, and vice versa. The experimental procedures to study the temperature-dependent characteristics of the hysteresis loops are described as follows: (i) the initial heat is acquired, after a short time of 5 A DC current is applied to the excitation coil of the magnetostrictive actuator; (ii) the magnetostrictive actuator cools naturally without input current, while the temperature on a surface spot of the magnetostrictive actuator is measured with a radiation infrared thermometer. It is noted that the actual temperature inside the magnetostrictive actuator is higher than the measured.

Fig. 2(b) shows the measured and fitting curves of the temperature vs. time and displacement vs. time respectively. The displacement is a relative quantity of which the initial value is set to a certain value. From Fig. 2(b), it can be seen that the displacement of the magnetostrictive micropositioner decreases as the surrounding temperature declines. The exact displacement vs. temperature model is not discussed because it is out of scope for this work. Then the 6 Hz sinusoidal motion experiment of the magnetostrictive micropositioner is conducted. Similarly, the initial temperature is obtained by providing a short time of DC current to the electromagnetic coil of the magnetostrictive actuator. During the experiment, the measured temperatures are 42.5 °C at initial time, 38.6 °C at 4 min, and 30.4 °C at 14 min. From Fig. 2(c), we see that the displacement of the micropositioner decreases from 200 mm to 125 mm when the temperature drops. The corresponding hysteresis loops vary in terms of the shapes and orientations, as shown in Fig. 2(d).

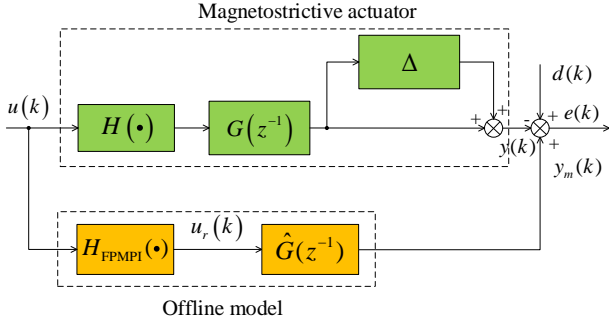


**Fig. 3.** Block diagram of the output vs. input offline identification approach for magnetostrictive actuator.

### 3. Hysteresis offline identification approach

The Hammerstein-based offline identification approach is used to describe the complicated output vs. input loops of magnetostrictive actuator.

As shown in Fig. 3, it is assumed that the magnetostrictive actuator comprises the rate-independent and rate-dependent subsystems respectively, that is,  $H(\cdot)$  and  $G(z^{-1})$ . The subsystems can be identified offline with the polynomial modified Prandtl Ishikii and linear time invariant dynamics models, that is,  $H_{\text{FPMPI}}(\cdot)$  and  $\hat{G}(z^{-1})$  respectively. However, if there exist some uncertainty in magnetostrictive actuator, for example, multiplicative uncertainty  $\Delta$  in Fig. 3, the hysteresis offline identification accuracy will be reduced. Meanwhile, if the external disturbances  $d(k)$ , e.g., aforementioned surrounding temperature, affect the output of the magnetostrictive actuator, the offline identified model cannot capture the disturbance-induced hysteresis variation.

The FPMPI model  $H_{\text{FPMPI}}(\cdot)$  is utilized to describe the rate-independent hysteresis. The FPMPI model is the cascade of the weighted fractional order polynomials superposition and weighted Play operators superposition. The structure of FPMPI model is similar to that of PMPI model in Ref. [8], but FPMPI model is more capable of capturing the hysteresis asymmetric behavior.

Since the displacement of the magnetostrictive actuator covers positive range, the single-side Play operator is used in this article. Its discrete form, at time instant  $k$ , can be expressed as

$$H_{r_H}[v](k) = \begin{cases} \max\{v(k) - r_H, \min\{v(k), H_{r_H}[v](k-1)\}\}; & k \geq 1 \\ \max\{v(0) - r_H, \min\{v(0), H_{r_H}[v](0)\}\}; & k = 0 \end{cases} \quad (1)$$

where  $v$  and  $H_{r_H}$  are the input and output of the Play operator respectively;  $H_{r_H}[0]$  is the initial value which is often set to 0, and  $r_H$  is the threshold value of Play operator. PI model is formulated with the weighted Play operator

superposition as

$$H[v](k) = \mathbf{H}_{r_H}[v](k) \cdot \mathbf{w}_H^T \quad (2)$$

where  $\mathbf{H}_{r_H} = [H_{r_H,0}, H_{r_H,1}, \dots, H_{r_H,N}]$  is the Play operator vector,  $\mathbf{w}_H = [w_{H,0}, w_{H,1}, \dots, w_{H,N}]$  is the weight vector.

$\mathbf{r}_H = [r_{H,0}, r_{H,1}, \dots, r_{H,N}]^T$  is the threshold vector corresponding to the Play operator vector, and its element is given by

$$r_{H,i} = \frac{i}{N+1} \max\{|v(k)|\}; \quad i = 0, 1, \dots, N. \quad (3)$$

The mathematical formulation of FPMPI model is given as

$$u_r(k) = \mathbf{H}[u](k) = \mathbf{H}_{r_H}[\mathbf{P}[u] \cdot \mathbf{w}_P^T](k) \cdot \mathbf{w}_H^T \quad (4)$$

where  $u(k)$  and  $u_r(k)$  are the FPMPI model input and output respectively,  $\mathbf{H}$  is the FPMPI model,  $\mathbf{P}[u] = [u^0, u^1, u^2, u^{1/2}, u^{L-1}, u^{1/(L-1)}]$  is the polynomial operator vector,  $\mathbf{w}_P = [w_{P,0}, w_{P,1}, w_{P,2}, \dots, w_{P,2L-2}]$  is the weight vector of the polynomial operator. A discrete transfer function is utilized for dynamics identification. The specified structure of the transfer function is formulated as

$$\hat{G}(z^{-1}) = z^{-d} \frac{\sum_{j=1}^J b_j z^{-j}}{1 + \sum_{i=1}^I a_i z^{-i}} \quad (5)$$

where  $d = 1$ ,  $a_i (i = 1 \dots I)$  and  $b_j (j = 1 \dots J)$  are the elements of the coefficient vectors. As shown in Fig. 3, with the intermediate signal  $u_r$  and output displacement  $y$ , the parameters of discrete transfer function are estimated offline.

### 4. Hysteresis online identification approach

We assume that the rate/temperature-dependent effect can be described by linear time variant system. As a result, the fixed coefficients of Model (5) are corrected to the time variant.

The block diagram of the proposed hysteresis online identification approach is shown in Fig. 4. First, the rate-independent nonlinear part  $H(\cdot)$  is modeled via the FPMPI model, thus the input is redefined to  $u_r$  and the system can be regarded as linear. Then, the linear dynamics is modeled with the OIIR filter whose parameters are estimated by the adaptive RLS algorithm.

The dynamics of the magnetostrictive actuator is constructed by the OIIR filter. The structure of the OIIR filter is shown as

$$\hat{G}(z^{-1}, k) = \frac{Y_m(z^{-1}, k)}{U_r(z^{-1}, k)} = \frac{P(z^{-1}, k)}{1 - Q(z^{-1}, k)} \quad (6)$$

where  $Y_m(z^{-1}, k)$  and  $U_r(z^{-1}, k)$  are the Z-transforms of the output and input of the actuator dynamics respectively;  $P(z^{-1}, k) = \sum_{i=0}^M p_i(k) z^{-i}$ ,  $Q(z^{-1}, k) = \sum_{j=1}^N q_j(k) z^{-j}$ ;  $p_i(k)$  and  $q_j(k)$  are the time variant numerator and denominator coefficients of the OIIR filter—these

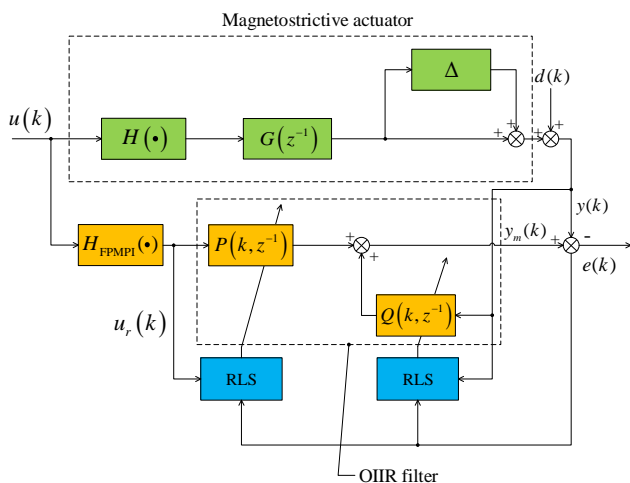


**Fig. 4.** Block diagram of output vs. input online modeling approach for the magnetostrictive actuator.

coefficients are also called OIIR filter weights;  $M + 1$  and  $N + 1$  are the numerator and denominator orders of the OIIR filter.

Therefore, the identification error  $e(k)$  is formulated as

$$e(k) = y(k) - \mathbf{w}^T(k) \boldsymbol{\varphi}(k) \quad . \quad . \quad . \quad . \quad . \quad . \quad . \quad . \quad (7)$$

where

$$\boldsymbol{\varphi}(k) = [u_r(k), \dots, u_r(k-M), y(k-1), \dots, y(k-N)]^T. \quad (8)$$

The weight vector  $\mathbf{w}(k)$  is estimated by minimizing the least-square error  $\xi(n)$  at time instant  $n$  as

$$\min \xi(n) = \sum_{i=0}^n \lambda^{n-i} e^2(i). \quad (9)$$

where  $\lambda$  ( $0 < \lambda \leq 1$ ) is the “forgetting factor” that makes the older error sequences exert less influence upon optimization process.

This minimization problem can be solved by the recursive least squares (RLS) technique, and the weight auto-tuning process is given as

$$\begin{aligned} \mathbf{P}(n+1) &= \frac{1}{\lambda} \left[ \mathbf{P}(n) - \frac{\mathbf{P}(n) \boldsymbol{\varphi}(n) \boldsymbol{\varphi}^T(n) \mathbf{P}(n)}{\lambda + \boldsymbol{\varphi}^T(n) \mathbf{P}(n) \boldsymbol{\varphi}(n)} \right] \\ \mathbf{w}^T(n+1) &= \mathbf{w}^T(n) + \mathbf{P}(n+1) \boldsymbol{\varphi} e(n). \end{aligned} \quad (10)$$

where  $\mathbf{P}(n)$  is the inverse of the correlation matrix  $\mathbf{R}(n)$  of the input sequence  $\mathbf{u}_r(n)$ . The initial value of matrix  $\mathbf{P}(n)$  is set to the inverse of the input signal power estimate. When the vector  $\mathbf{w}(n)$  converges to be constant, the IIR-based dynamics is achieved. By finding the roots of the characteristics polynomial, the stability of IIR model can be determined.

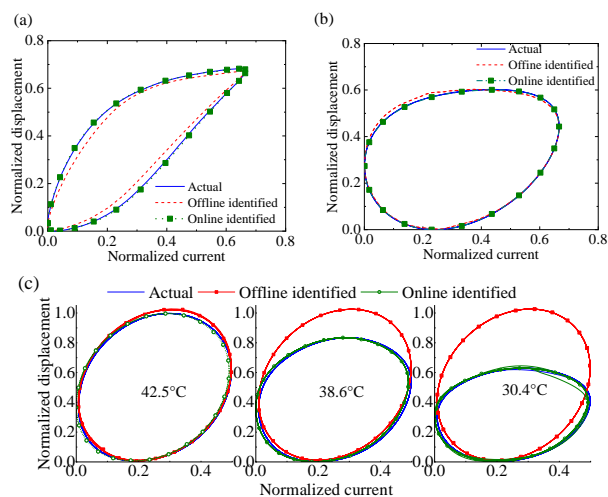


**Fig. 5.** Comparison of the actual, offline and online identified rate-dependent hystereses for (a) 1 Hz and (b) 5 Hz input currents; (c) comparison of the actual, offline and online identified temperature-dependent hystereses.

## 5. Hysteresis offline and online identification results

To identify the rate-independent hysteresis, the 0.05 Hz sinusoidal currents of which the amplitudes increase arithmetically from 0.3 A to 3 A are applied to drive the magnetostrictive actuator. The measured currents and displacements are normalized to 3 A and 37  $\mu\text{m}$  respectively, which is performed for all experimental data. With the measured input/output data and FPMPI model in Eq. (4), the weight coefficients of Play and fractional order polynomial operators,  $\mathbf{w}_H$  and  $\mathbf{w}_P$ , are obtained. The orders of  $\mathbf{w}_H$  and  $\mathbf{w}_P$  are set 10 and 8 respectively with the trade-off between identification accuracy (more than 97%) and computational complexity (to keep low).

To identify the transfer function of the magnetostrictive actuator offline, the small amplitude and 0.1–20 Hz band-limited current is utilized to drive the actuator. To keep relatively low computation complexity and small identification error (<3%), the numerator and denominator orders of the transfer function, Eq. 5, are selected as 8 and 4, and the delay constant is set to 1 with trial and error.

For the OIIR filter, the weights are identified online according to different input signals and surrounding temperatures.

The actual, offline and online identified rate/temperature-dependent hystereses of the magnetostrictive actuator are comparatively illustrated in Fig. 5. Fig. 5(a) and Fig. 5(b) correspond to the cases of 1 Hz and 5 Hz input currents respectively. It is observed that although the actual hysteresis loop shapes of the magnetostrictive actuator change dramatically, the identified hysteresis loops can adapt to the variation of the actual ones. The relative identification errors of 1 Hz and 5 Hz hystereses are 5.16% and 2.29% respec-

tively in Norm-2 sense. However, the uncertainty in magnetostriuctive actuator is not considered for hysteresis offline identification approach. By using hysteresis online identification approach, the relative identification errors are reduced to 0.02% and 0.01%.

Fig. 5(c) compares the actual, offline and online identified temperature-dependent hysteresis curves. When the surrounding temperature decreases from 42.5 °C to 30.4 °C, the thermal-induced strain of the magnetostriuctive material decreases and the shapes of hysteresis loops change. Whereas, the offline identified hysteresis model can not track this change. The relative identification errors are 3.43%, 21.06%, and 58.12% for the 42.5 °C, 38.6 °C, and 30.4 °C cases. By contrast, those values are reduced to 0.04%, 0.03%, and 0.08% via the proposed hysteresis online identification approach.

## 6. Conclusion

In this article, we report a FPMPI and OIIR integrated model to online identify the rate/temperature-dependent hystereses for the magnetostriuctive actuator. The custom-developed magnetostriuctive actuator are employed to verify the proposed hysteresis online identification approach. First of all, the complicated variations of the rate/temperature-dependent hystereses are analyzed experimentally. The traditional Hammerstein-based offline identification approach is introduced. However, the system uncertainty and external disturbance are not considered for the hysteresis offline identification approach. Then, instead of the offline transfer function, we apply an OIIR filter to capture the dynamic variations of the rate/temperature-dependent hysteresis loops. According to the experimental result comparison between the offline and online approaches, it is found that all hysteresis online identification results are better significantly than the offline ones under different input currents and surrounding temperatures. In the future, we will further develop the hysteresis online identification approach by constructing an online FPMPI model and integrating it with the OIIR filter.

## Acknowledgements

The work is supported by Shanghai Sailing Program (20YF1417400), Postdoctoral Science Foundation of China (2021M692022), Natural Science Foundation of Shanghai (19ZR1474000), National Key R&D Program of China (2016YFB0501003), National Nature Science Foundation of China (61803258), for which the authors are most grateful. The authors also thank Prof. Bintang Yang in Shanghai Jiao Tong University for providing experimental devices.

## References

- [1] L. Sun, F. Chen, and W. Dong, "A PZT actuated 6-dof positioning system for space optics alignment," *Flight control and detection*, no. 4, pp. 1–13, 2019.
- [2] P. Chen, X.-X. Bai, L.-J. Qian, and S.-B. Choi, "An approach for hysteresis modeling based on shape function and memory mechanism," *IEEE/ASME Transactions on Mechatronics*, vol. 23, no. 3, pp. 1270–1278, 2018.
- [3] Y.-J. Liu, S. Tong, C. P. Chen, and D.-J. Li, "Neural controller design-based adaptive control for nonlinear mimo systems with unknown hysteresis inputs," *IEEE transactions on cybernetics*, vol. 46, no. 1, pp. 9–19, 2015.
- [4] Z. Li, J. Shan, and U. Gabbert, "Inverse compensation of hysteresis using krasnoselskii-pokrovskii model," *IEEE/ASME Transactions on Mechatronics*, vol. 23, no. 2, pp. 966–971, 2018.
- [5] L. Fang, J. Wang, and Q. Zhang, "Identification of extended hammerstein systems with hysteresis-type input nonlinearities described by preisach model," *Nonlinear dynamics*, vol. 79, no. 2, pp. 1257–1273, 2015.
- [6] M. Rakotondrabe, "Multivariable classical prandtl-ishlinskii hysteresis modeling and compensation and sensorless control of a nonlinear 2-dof piezoactuator," *Nonlinear Dynamics*, vol. 89, no. 1, pp. 481–499, 2017.
- [7] Y. Qin, Y. Tian, D. Zhang, B. Shirinzadeh, and S. Fatikow, "A novel direct inverse modeling approach for hysteresis compensation of piezoelectric actuator in feedforward applications," *IEEE/ASME Transactions on Mechatronics*, vol. 18, no. 3, pp. 981–989, 2013.
- [8] S. Yi, B. Yang, and G. Meng, "Ill-conditioned dynamic hysteresis compensation for a low-frequency magnetostriuctive vibration shaker," *Nonlinear Dynamics*, vol. 96, no. 1, pp. 535–551, 2019.
- [9] M. Al Janaideh, S. Rakheja, and C.-Y. Su, "A generalized prandtl-ishlinskii model for characterizing the hysteresis and saturation nonlinearities of smart actuators," *Smart Materials and Structures*, vol. 18, no. 4, p. 045001, 2009.
- [10] M. Kciuk, K. Chwastek, K. Kluszczyński, and J. Szczygłowski, "A study on hysteresis behaviour of sma linear actuators based on unipolar sigmoid and hyperbolic tangent functions," *Sensors and Actuators A: Physical*, vol. 243, pp. 52–58, 2016.
- [11] M. Al Janaideh and O. Aljanaideh, "Further results on open-loop compensation of rate-dependent hysteresis in a magnetostriuctive actuator with the prandtl-ishlinskii model," *Mechanical Systems and Signal Processing*, vol. 104, pp. 835–850, 2018.
- [12] S. Xiao and Y. Li, "Modeling and high dynamic compensating the rate-dependent hysteresis of piezoelectric actuators via a novel modified inverse preisach model," *IEEE Transactions on Control Systems Technology*, vol. 21, no. 5, pp. 1549–1557, 2013.
- [13] O. Aljanaideh, M. Al Janaideh, S. Rakheja, and C.-Y. Su, "Compensation of rate-dependent hysteresis nonlinearities in a magnetostriuctive actuator using an inverse prandtl-ishlinskii model," *Smart Materials and Structures*, vol. 22, no. 2, p. 025027, 2013.
- [14] P.-K. Wong, Q. Xu, C.-M. Vong, and H.-C. Wong, "Rate-dependent hysteresis modeling and control of a piezostage using online support vector machine and relevance vector machine," *IEEE Transactions on Industrial Electronics*, vol. 59, no. 4, pp. 1988–2001, 2011.
- [15] D. Zhang, M. Jia, Y. Liu, Z. Ren, and C.-S. Koh, "Comprehensive improvement of temperature-dependent jiles-atherton model utilizing variable model parameters," *IEEE Transactions on Magnetics*, vol. 54, no. 3, pp. 1–4, 2017.
- [16] P. Li, F. Yan, C. Ge, X. Wang, L. Xu, J. Guo, and P. Li, "A simple fuzzy system for modelling of both rate-independent and rate-dependent hysteresis in piezoelectric actuators," *Mechanical Systems and Signal Processing*, vol. 36, no. 1, pp. 182–192, 2013.
- [17] H.-T. Zhang, B. Hu, L. Li, Z. Chen, D. Wu, B. Xu, X. Huang, G. Gu, and Y. Yuan, "Distributed hammerstein modeling for cross-coupling effect of multiaxis piezoelectric micropositioning stages," *IEEE/ASME Transactions on Mechatronics*, vol. 23, no. 6, pp. 2794–2804, 2018.
- [18] S. Yi, B. Yang, and G. Meng, "Microvibration isolation by adaptive feedforward control with asymmetric hysteresis compensation," *Mechanical Systems and Signal Processing*, vol. 114, pp. 644–657, 2019.
- [19] X. Tan and J. S. Baras, "Modeling and control of hysteresis in magnetostriuctive actuators," *Automatica*, vol. 40, no. 9, pp. 1469–1480, 2004.
- [20] M. Al Janaideh, M. Al Saaideh, and M. Rakotondrabe, "On hysteresis modeling of a piezoelectric precise positioning system under variable temperature," *Mechanical Systems and Signal Processing*, vol. 145, p. 106880, 2020.
- [21] R. Köhler and S. Rinderknecht, "A phenomenological approach to temperature dependent piezo stack actuator modeling," *Sensors and Actuators A: Physical*, vol. 200, pp. 123–132, 2013.
- [22] Z. Zheng, J. Lin, H. Kong, F. He, Y. Peng, and L. Chen, "Missile elastic vibration identification and adaptive suppression," *Flight control and detection*, no. 6, pp. 41–47, 2019.